

# Metop long term free-dynamics attitude analysis, for improved re-entry prediction

By Stefano PESSINA<sup>1</sup>, Pierluigi RIGHETTI<sup>1</sup>,  
João BRANCO<sup>2</sup>, Victor Manuel MORENO VILLA<sup>3</sup>, Thomas Vincent PETERS<sup>3</sup>

<sup>1</sup> EUMETSAT, Darmstadt, Germany

<sup>2</sup> GMV, Lisbon, Portugal <sup>3</sup> GMV, Madrid, Spain

(Received April 17th, 2017)

For a LEO spacecraft, the long term (>25 years) orbit re-entry propagation are typically performed assuming random tumbling, decoupling the attitude dynamics, and using a mean area for the perturbation depending on external surfaces. Due to its mass properties, especially at higher altitude in the initial part of the decay, the EUMETSAT mission Metop can have a stable attitude configuration, due to the predominant effect of the gravity gradient with respect to air drag. The knowledge of the attitude evolution around eventual temporally stable configuration allows the definition of more accurate mean cross-section area for decay analysis, and therefore an improved re-entry prediction. A dedicated attitude dynamics simulator (based on ECSS standard models) has been used by the EUMETSAT flight dynamics team to perform a sensitivity analysis of the stability, based on initial spacecraft attitude, lock position of the solar array with respect to satellite body, orbital altitude, solar activity, orbital plane orientation with respect to the Sun. This paper reports on the modelling assumptions, assumed simulation inputs, stability results and subsequent characterization of the mean cross-section area in support to re-entry long term propagation and end-of-life strategy selection.

**Key Words:** LEO, End-of-Life, Attitude Dynamics, Re-entry

## Nomenclature

EPS	: EUMETSAT Polar System
Metop	: Meteorological Operational satellite
LEO	: Low Earth Orbit
GBF	: Geometrical Body Frame
SA	: Solar Array
Cd	: Drag Coefficient
A	: Cross-section area (wrt relative wind)
EOL	: End-Of-Life
LTAN	: Local Time of Ascending Node

## 1. Introduction, EUMETSAT and Metop

EUMETSAT is the “EUropean organisation for the exploitation of METeorological SATellites”. It is an independent intergovernmental organisation created in 1986 to establish, maintain and exploit European systems of operational meteorological satellites. It currently operates a system of meteorological satellites, monitoring the atmosphere and ocean and land surfaces which deliver weather and climate-related satellite data, images and products – 24 hours a day, 365 days a year.<sup>1</sup> EUMETSAT currently has eight operational weather satellites. Meteosat-7, -8, -9, -10, -11, Jason-3, and Metop-A, -B. Meteosat are the satellites of the geosynchronous fleet. Jason-3 delivers oceanographic data from not-Sun-synchronous Low-Earth-Orbit (LEO) at 1336km altitude.

Metop are the LEO polar meteorological satellites<sup>2</sup>, which form the space segment component of the overall EUMETSAT Polar System (EPS). Metop-A (launched in 2006) and Metop-B (launched in 2012) are also in a LEO polar orbit, at an altitude of 817 kilometres; the operational

orbit is Sun-synchronous, with Local Time of Ascending node at 21:30. The two satellites currently operate in parallel for users’ benefit. Metop-C is planned to be launched in 2018.

Fig. 1 shows the Metop spacecraft and the Geometrical Body Frame (GBF). In routine operations  $Z_{GBF}$  is kept pointing towards the Earth (nadir),  $Y_{GBF}$  pointing parallel to the orbit normal and  $X_{GBF}$  forming a right-handed triad, thus pointing towards the orbital velocity (with oscillations due to orbit eccentricity or activation of yaw steering mode). This guidance is kept also for executing in-plane manoeuvres, while out-of-plane are performed with  $\sim 90^\circ$  Yaw rotation around  $Z_{GBF}$ .

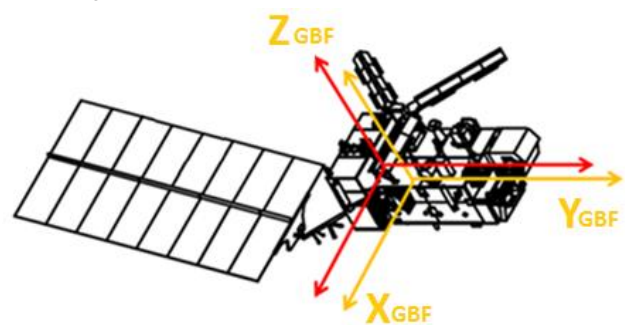


Fig. 1: Metop spacecraft, Geometric Body frame in gravity centre

Metop-A, after 10 years of operations controlling his orbital plan orientation, executed its last out-of-plane manoeuvre on August 2016. The final part of the Metop-A mission, after the nominal lifetime, is divided in 3 consecutive phases that required extensive Flight Dynamics analysis:

- Mission extension
- End-of-life (EOL) manoeuvres
- Orbit decay after EOL manoeuvres

The first 2 will be briefly introduced in the next section, for information only. The focus of this paper is the 3<sup>rd</sup> phase.

## 2. Metop mission extension, End-of-life manoeuvres

After nominal mission lifetime, during an extension phase before re-orbiting<sup>8</sup>, Metop-A continues providing operational data, but it starts to drift out of the nominal orbit plane. The Local Time of Ascending Node (LTAN) will change from the value of 21:30, lowering progressively to 19:40 in early 2022. In this phase, the solar array is kept rotating, to maximize the sun exposure. Due to LTAN drift, there will be change to the sun illumination (reducing the eclipse time) and the sun incidence, both on the solar array (thus changing available power on-board) and satellite body, also due to shadowing: after 40 minutes of LTAN Drift, the Solar Array will start shading the battery radiator, that is located on the face of the satellite, hosting the Solar Array hinge.

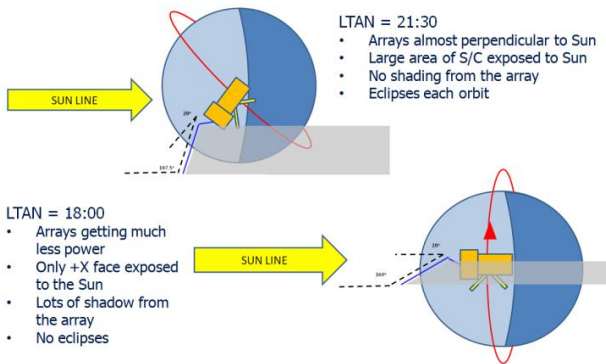


Fig. 2. Sun incidence changes due to LTAN drift

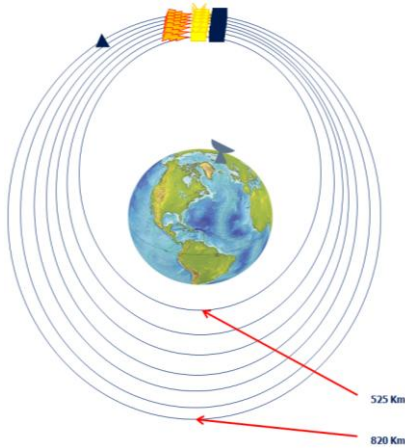


Fig. 3. EOL maneuver sequence for perigee lowering at South Pole

In the 2<sup>nd</sup> phase, starting from a nearly circular operational orbit with ~820 km radius, the current EOL strategy foresees a progressive perigee lowering above the South pole, until ~20 kg of fuel remains. The apogee at North Pole helps operations during passivation<sup>3</sup>, while the long burns (~30 mins) mean that the apogee lowers too during this manoeuvres campaign, clearing the operational orbit. Target is to reach 550km perigee height that will be lowered further in case of still available fuel reserves (525km is the hard limit, for proper functioning of Earth sensors and wheels de-saturation by magnetorquers).

In these 2 mission phases, dedicated analysis were performed by the EUMETSAT Flight Dynamics team, both to study the evolution of the solar panel shadowing on the solar array in the first phase<sup>8</sup>, to evaluate the wheels saturation level due to increased air-drag after EOL manoeuvres in nominal attitude<sup>9</sup>, but also to perform special operations, like pitch-over manoeuvres to inertial pointing<sup>10</sup>.

## 3. Orbit decay after EOL manoeuvres

At the end of the manoeuvres, the spacecraft will be passivated. After the AOCS deactivation, the attitude will evolve in free dynamics, with the solar array locked in a fixed position.

The air density rises exponentially as altitude reduces, so the successive apogee lowering is naturally obtained by aerodynamic drag, with the apogee height lowering progressively till a circular decay orbit is reached. In this phase, the perigee position will rotate continuously with respect to the Earth, with a full 360 deg rotation roughly every 4 months. In addition, the LTAN will also change progressively, spanning all values between 00:00 and 24:00.

In line with international debris mitigation guidelines ISO24113, a target a re-entry of the satellite within 25 years was initially verified by EUMETSAT using the CNES-STELA software<sup>4</sup>: the tool was configured assuming random tumbling of the spacecraft, with a simplified shape model formed by 6.319m x 2.5m x 2.712m parallelepiped (external envelop), with a 20° inclined solar panel of 8.174m x 4.972m surface.

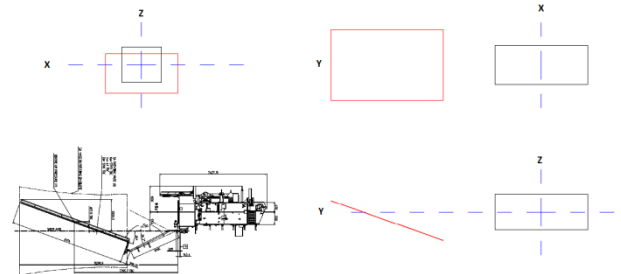


Fig. 4. Metop spacecraft (YZ view, bottom left) and cuboid+panel model

According to this model (see Fig. 4), the projected area in the X, Y, Z direction and the random tumbling equivalent cross-section area have been computed, both considering the Solar Array (SA) in the so called canonical position and with a 90° rotation with respect to that position; the results are shown in Table 1.

Table 1. Projected mean cross-section area

Orientation	SA Rotation	Mean Area	SA Rotation	Mean Area
Fixed-X	0°	15.74m <sup>2</sup>	90°	54.04m <sup>2</sup>
Fixed-Y	0°	15.34m <sup>2</sup>	90°	14.12m <sup>2</sup>
Fixed-Z	0°	55.10m <sup>2</sup>	90°	16.95m <sup>2</sup>
Random tumbling	0°	39.71m <sup>2</sup>	90°	39.79m <sup>2</sup>

A reference long term orbit propagation was run then, using drag coefficient Cd=2.0 and cross-section area of 34.00m<sup>2</sup> (for

15% conservative margin on the random tumbling value, also because the projected area have been computed with external envelop). Start date was 2022/01/01 in line with the current EOL plan for Metop-A; results are reported in Fig. 5 , Fig. 6.

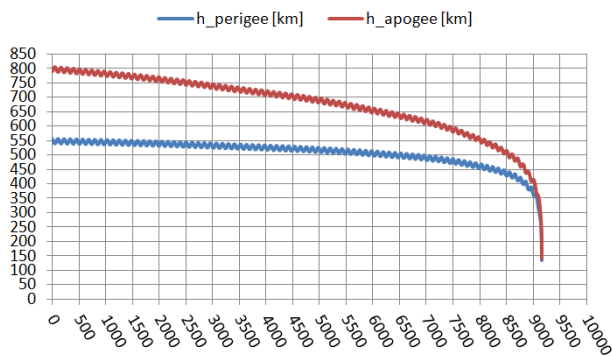


Fig. 5 Orbit decay after EOL manoeuvres, apogee/perigee height, as function of elapsed time in days

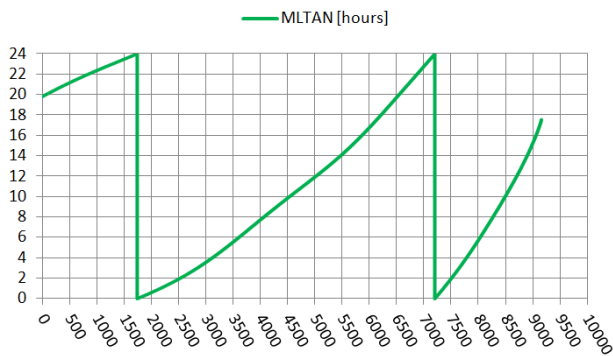


Fig. 6. Orbit decay after EOL manoeuvres: Mean LTAN evolution, as function of elapsed time in days

#### 4. Models for free-attitude dynamics

To model the dynamics in orbit decay phase, an accurate dynamics simulator was used, called AADD, standing for Analysis of Attitude Dynamics and Disturbance<sup>5)</sup>, developed by GMV under EUMETSAT contract. The disturbances torques modelled in this are indicated in Table 2 , also showing compliance with respect to ECSS space environment standard<sup>6)</sup> and the other relevant models<sup>7)</sup>.

Table 2. Models in AADD simulator

Environment	Model
Sun Constant	Compliant with standard <sup>6)</sup>
Atmosphere	Compliant with standard <sup>6)</sup> , NRLMSISE-00 model
Magnetic field	Compliant with standard <sup>6)</sup> , IGRF-10 model
Ephemerides	Compliant with standard <sup>6)</sup> , DE405 JPL
Disturbance Torque	Model
Gravity gradient	From literature <sup>7)</sup> , Earth assumed point mass
Magnetic	From literature <sup>7)</sup> , satellite as single dipole
SunRadiation Press.	From literature <sup>7)</sup> , satellite 3D mesh model
Aerodynamic	From literature <sup>7)</sup> , satellite 3D mesh model
Others	Model
Wind	Co-rotating atmosphere(fixed with the Earth)
Shadowing	Considered using satellite 3D mesh model
Shear stress	Considered using satellite 3D mesh model

Both the Sun Radiation Pressure and Aerodynamic disturbance depend on the geometry of the spacecraft and the respective tiles, with contribution to total forces and torques computed according to the tiles relative illumination by the Sun or the local wind, at each simulation step. The solar panel(s) can be rotated, changing the geometry along the simulation (mesh updated at every simulation step, in case of moving Solar Array). Sun and Moon eclipses and their effects on radiation pressure are modelled considering the celestial body as spherical. An example of 3D mesh is shown in Fig. 7

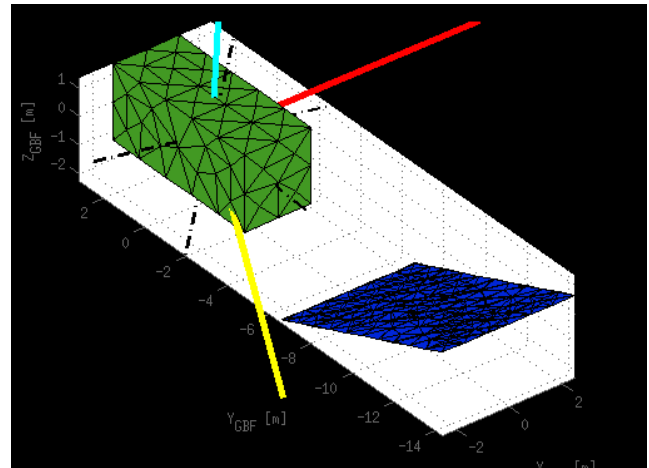


Fig. 7. Example of 3D mesh.

red line = orbital velocity, light blue line = radial direction (nadir), yellow line = Sun direction, black = Principal Axes of Inertia

The computation of the total inertia is done using the Huygens-Steiner theorem, summing up the contribution of the central body and the solar array, according to its orientation.

The Aerodynamic model is sophisticated, thanks to its heritage from studies within ESA very low-earth orbit mission GOCE (down to 250 km altitude). The drag acceleration is computed (according to the relative wind) using the model of Schaaf/Chambre (modification of the Maxwell model, introducing the accommodation coefficients). Two other effects are taken into account, not specified in the ECSS, shadowing and shear stress: the former changes the effective area, and the latter introduces spurious tangential components to the disturbances forces (and consequent torques).

#### 5. Simulation scenarios

To study the evolution of Metop attitude while in free-dynamics (no active closed-loop attitude control), it is foreseen to run a sequence of simulations: purpose is to characterize the dynamics evolution, with identification of stable or partially stable configurations, as difference from the initial simplified assumption of random tumbling. Inputs for this are 8 orbits at different perigee/apogee height (taken as snapshots at different Mean LTAN, from the decay propagation, shown in Fig. 5, Fig. 6.) see Table 3. Each simulation covers 6 full orbits, according to the orbital period.

Table 3. Orbit scenarios for AADD simulations

Orbit scenario	Date [yyyy/mm/dd]	MLTAN [hours]	Perigee Height [km]	Apogee Height [km]
1	2022/01/01	19.80	555.86	789.86
2	2028/12/03	02.00	539.64	746.46
3	2033/02/15	08.00	525.58	712.52
4	2036/12/22	14.00	504.20	681.71
5	2039/12/02	20.00	498.37	632.95
6	2042/07/18	02.00	484.52	581.21
7	2044/08/17	08.00	448.10	533.10
8	2046/05/07	14.00	385.20	443.92

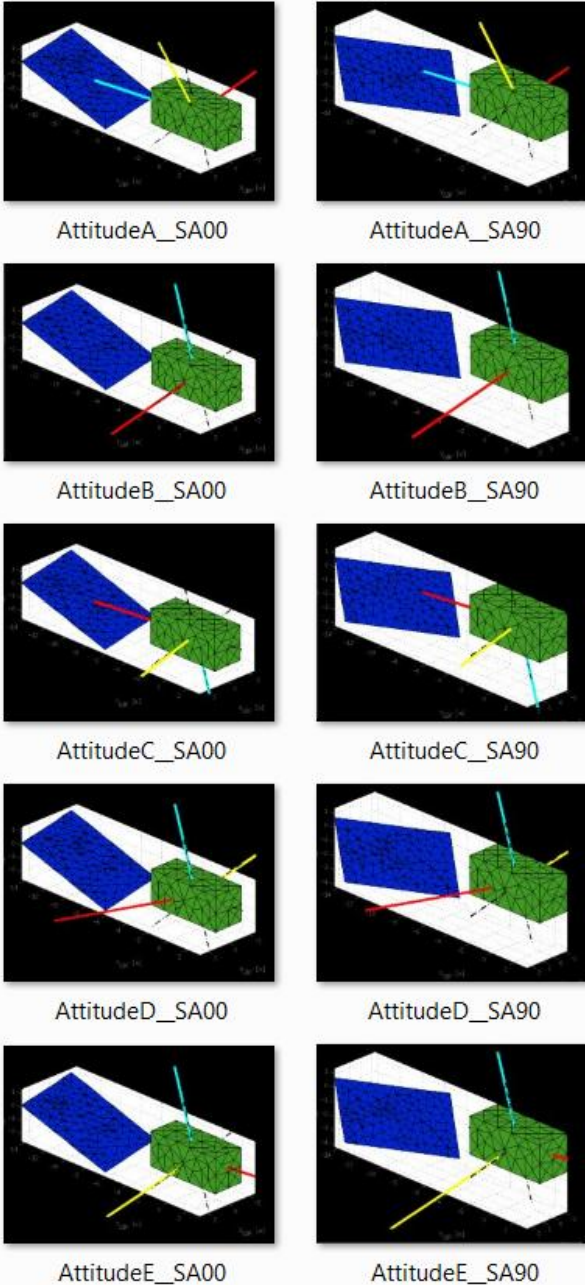


Fig. 8. Attitude scenarios in body frame: red line = orbital velocity, light blue line = radial direction (nadir), yellow line = Sun direction (orbit scenario 1)

The selected attitude scenarios are 8, as shown in the first column of Fig. 8, labelled “A” to “E”: the body-frame

orientation in inertial space is changed to have different configuration of the radial and relative wind direction. In addition, each of this attitude scenarios is repeated, but rotating the Solar Array of  $90^\circ$  (see 2<sup>nd</sup> column of the same picture). As shown in Fig. 7, the principal axes of inertia of the spacecraft are rotated about  $10^\circ$  around the solar panel rotation axis with respect to the geometric frame: to ease the simulation setup, the relative configurations for nadir, local wind and solar array rotation have been referred to the principal axis frame.

Another parameter of the simulation is the solar activity: for this, 2 different levels are considered, as representative of the maximum and minimum of a Solar Cycle, with the following 10.7-cm Solar Radio Flux (F10.7) and geomagnetic (daily) index of Planetary Equivalent Amplitude (Ap):

- High Solar activity:  $F10.7 = 250$   $Ap=20$
- Low Solar activity:  $F10.7 = 75$   $Ap=10$

This gives 8 orbits x 10 attitude x 2 solar activities, so 160 simulations in total.

## 6. Individual simulation results examples

For each of these simulations, the whole attitude dynamics and kinematic evolution in time is simulated, saved and stored for post-processing. Among the various outputs, the evolution of the angular velocity in body fixed frame and with respect to the orbital velocity vector give indications about the stability of the solution, and the impact on the air drag. In general, the simulation can be classified as stable, partially stable or unstable. An example of simulation output is given in all the plots from Fig. 9 to Fig. 14, for an example-set of results, for each of the three mentioned categories. The plots on the left show the unit vector of the angular velocity in GBF frame, while those on the right the air drag factor  $Cd*A$ : the standard drag force definition is  $D = \frac{1}{2}\rho v^2 (C_d*A)$ , where  $v$  is the local wind (different from the orbital velocity),  $\rho$  the current atmospheric density, and  $Cd*A$  is the combination of drag coefficient and cross-section area. The AADD tool computes the 3D aerodynamic force as function of time during each simulation; this vector is scaled down by  $\frac{1}{2}\rho v^2$ ; the resulting vector is projected along the orbital velocity, to get the actual component of  $Cd*A$ , that is reducing the orbital energy.

The 1<sup>st</sup> row (Fig. 9, Fig. 10) shows a case of stable configuration: it can be seen that the angular velocity stays close to parallel to the axis of maximum inertia, while the axis of minimum inertia stay pointed towards the Earth. This is known to be a gravity gradient stable configuration. It’s interesting to note: for this level of low solar activity, the attitude is kept even when the Solar Array has a  $90^\circ$  rotation, this maximises the  $Cd*A$  (to  $111.71m^2$ , in line with Table 1, for a  $Cd$  slightly above 2) and therefore the re-entry time. Unfortunately this configuration cannot be forced at the beginning of the decay phase, because the spacecraft is designed to perform only yaw rotations, eventually moving the axis of minimum inertia in the plane orthogonal to nadir.

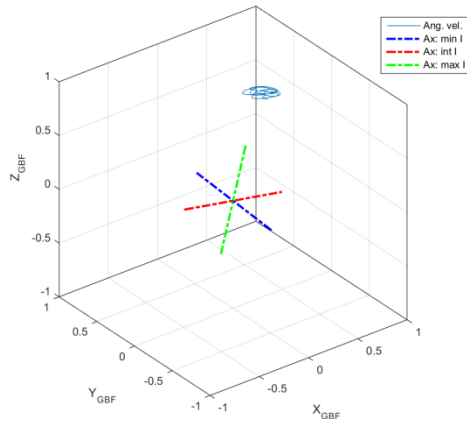


Fig. 9. Sim.scenario Orbit-3, Attitude-A, SA90, low solar activity: Angular Velocity unit vector & Principal Inertia axis in body frame GBF

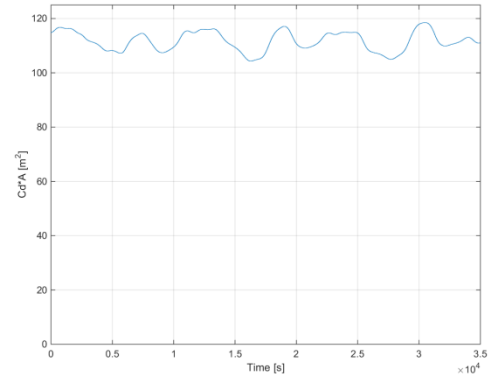


Fig. 12. Sim.scenario Orbit-3, Attitude-A, SA90, low solar activity: Cross Section Area times Drag coefficient ( $C_d \cdot A$ ) as function of time

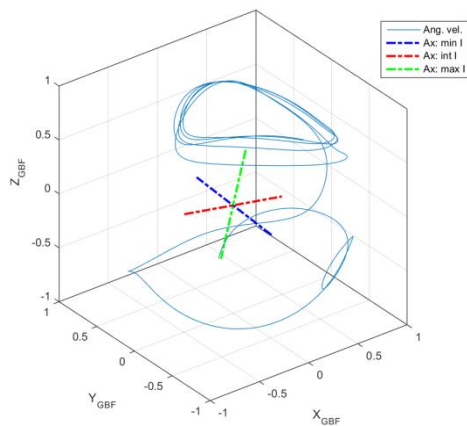


Fig. 10. Sim.scenario Orbit-3, Attitude-D, SA90, low solar activity: Angular Velocity unit vector & Principal Inertia axis in body frame GBF

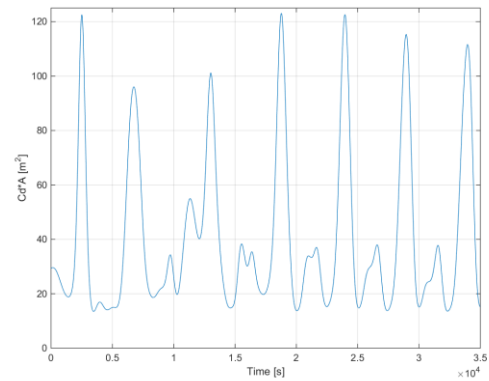


Fig. 13. Sim.scenario Orbit-3, Attitude-D, SA90, low solar activity: Cross Section Area times Drag coefficient ( $C_d \cdot A$ ) as function of time

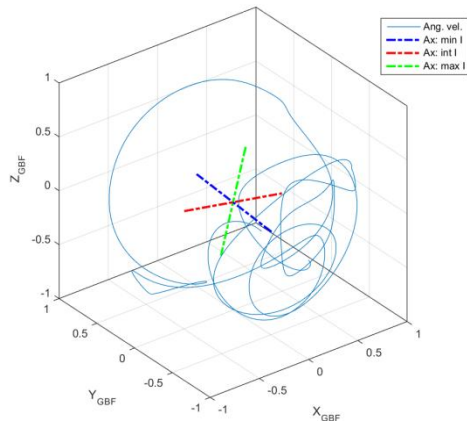


Fig. 11. Sim.scenario Orbit-3, Attitude-B, SA90, low solar activity: Angular Velocity unit vector & Principal Inertia axis in body frame GBF

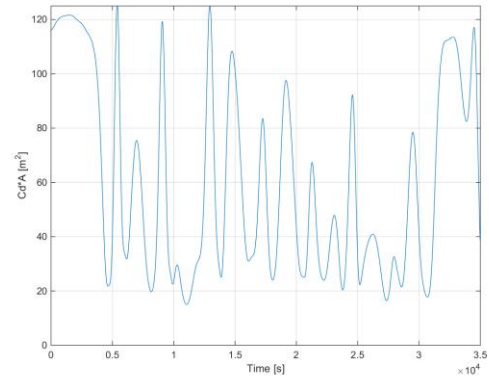


Fig. 14. Sim.scenario Orbit-3, Attitude-A, SA90, low solar activity: Cross Section Area times Drag coefficient ( $C_d \cdot A$ ) as function of time

The 2<sup>nd</sup> row (Fig. 11, Fig. 12) shows a partially stable case, when after initial tumbling, a flat spin is induced, causing the  $Cd^*A$  to have a mean value of  $18.98m^2$ . Scaling down for a  $Cd$  of 2, this is well below the random tumbling equivalent from Table 1.

The 3<sup>rd</sup> row (Fig. 13, Fig. 14) shows an unstable case, where the  $Cd^*A$  is  $60.48 m^2$ , which is close but anyway still slightly below random tumbling equivalent.

### 7. Summary of all results

The following pictures gives a summary of all simulated scenarios, showing the  $Cd^*A$  factor (y-axis) as function of the orbit case (x-axis), with colour-code according to the initial attitude (Fig. 15), to solar activity level (Fig. 16) and to the rotation of the solar array (Fig. 17).

As mentioned before, for low-solar activity and with rotation of  $90^\circ$  of the Solar Array (maximising drag), there is a family of stable solutions, due to gravity gradient stabilisation, in Attitude-A. These allows very high  $Cd^*A$  levels, in all orbit scenarios snapshots of the decay.

Another evident observation is that, when excluding the set related to Attitude-A, all results are below (in many cases well below)  $65m^2$ : this is due to multiple configurations in stable or partially stable flat-spin. This means they are below the  $Cd^*A$  for random tumbling, as computed at the beginning of the paper (that is  $79.5m^2$ , for an area of  $39.75$  and a  $Cd$  of 2).

Final consideration, a rotation of the solar array (to maximise the area exposed to the relative wind at the beginning of the simulation) has an overall de-stabilising effect, that could allow achieving an unstable spin configuration, therefore augmenting the overall drag level.

### 8. Conclusion

The final phase of Metop End-Of-Life will start after 2022, with a final phase of orbit decay, in free attitude dynamics. Its starting point was designed on basis of ISO24113, assuming random tumbling for the ballistic coefficient estimation.

An accurate attitude dynamics simulator has been developed and uses to verify a-posteriori the mean level of the ballistic coefficient in this phase, for various orbit size, initial attitude, solar activity level and spacecraft configuration.

The conclusion is that the assumption of random tumbling is not a conservative approach for the Metop spacecraft, because various stable or partially stable configurations were identified. Furthermore, to counter-react this, the selection of specific configurations (i.e. locking the solar array as part of the decommissioning, to maximise initial exposure to the relative wind) can augment the probability of dynamic instability and thus the air drag for re-entry.

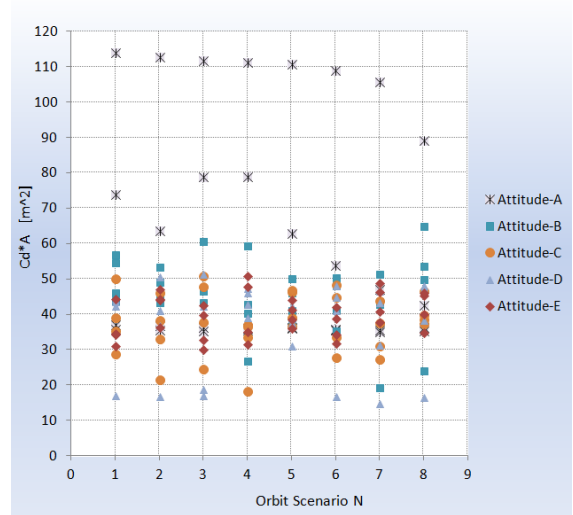


Fig. 15. Summary of all results: mean  $Cd^*A$  according to initial Attitude

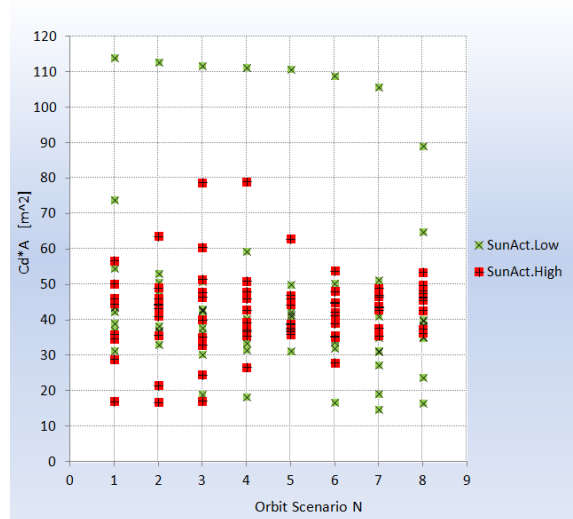


Fig. 16. Summary of all results: mean  $Cd^*A$  according to Solar Activity

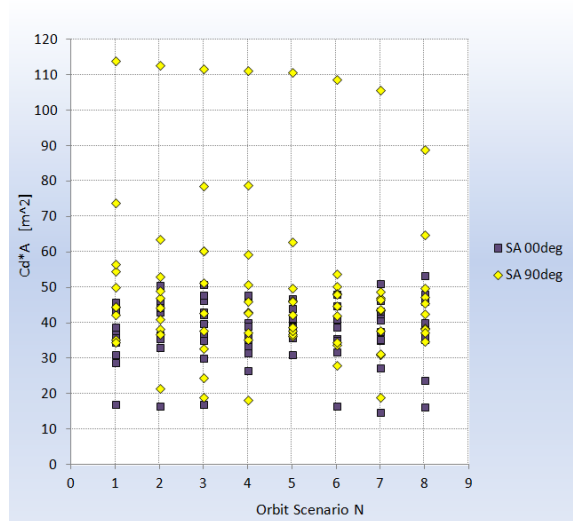


Fig. 17. Summary of all results: mean  $Cd^*A$  according to SA rotation

## References

- 1) EUMETSAT external web-site:  
[www.eumetsat.int](http://www.eumetsat.int)
- 2) Metop mission introduction page:  
<http://www.eumetsat.int/website/home/Satellites/CurrentSatellites/Metop/index.html>
- 3) Sancho F., Paulino T., de Juana J.M., Righetti P., METOP-A DE-ORBITING USING VERY LARGE IN-PLANE MANEUVERS, 2015 International Symposium of Space Flight Dynamics
- 4) Fraysse H., Morand V., Le Fevre C., Deleflie F., Wailliez S., Lamy A., Martin T., Perot E., LONG TERM ORBIT PROPAGATION TECHNIQUES DEVELOPED IN THE FRAME OF THE FRENCH SPACE ACT, 2011 International Symposium of Space Flight Dynamics
- 5) Pessina S., Gomes Paulino N.M.G., De Juana J.M., Righetti P.L., EUMETSAT STUDY FOR ATTITUDE DYNAMICS AND DISTURBANCES IN LEO AND GEO ENVIRONMENT, 2014 International Symposium of Space Flight Dynamics
- 6) ECSS Space Environment Standard, ECSS-E-ST-10-04C
- 7) Wertz J.R., SPACECRAFT ATTITUDE DETERMINATION AND CONTROL, SPRINGER
- 8) Righetti P.L., Dyer R., FEASIBILITY OF METOP-A MISSION EXTENSION ON DRIFTING LOCAL TIME, 2017 International Symposium of Space Flight Dynamics
- 9) AADD PHASE-3 WP4, METOP EOL ATTITUDE STUDY FINAL REPORT, GMV-EUM-AADD-EOL-FR Iss.01
- 10) Sancho F., Fischer J., Tarquini S., NON-NOMINAL ATTITUDE MANOEUVRES DURING METOP-A EXTENDED LIFETIME, 2017 International Symposium of Space Flight Dynamics